Control of Line Side Converter for Doubly Fed Induction Generator with Active Power Filter and Load Balancing

S. Wangsathitwong, S. Sirisumrannukul, S. Chatratana, and W. Deleroi

Abstract*— *A control system of line side converter for a doubly fed induction generator with active power filter and load balancing capability is presented. The control scheme is based on the model of the system on synchronously rotating reference frame (d-q axis). The d-q axis current components are used to control active power and reactive power, respectively. In this reference frame, the d-q current components of the nonlinear load are composed of dc and ac quantities. The dc component of d-axis current represents the fundamental of active current while ac components represents harmonic currents and unbalanced load currents. The q-axis current correspond to reactive power, harmonic currents and unbalanced load currents. The elimination of ac component of the d-axis current and q-axis current by appropriate compensation ensures that the converter is operating at unity power factor with active power filter function and load balancing capability. Simulation results of a line side converter with unbalanced nonlinear load confirm good performance of the proposed control method.

***Keywords*— Doubly fed induction generator, Line side converter, Active power filter, Load balancing.**

1. INTRODUCTION

Wind energy is one of the fastest growing renewable energy systems. Many large wind farms employ doubly fed induction generator (DFIG) with variable speed wind turbines [1]. More than 60% of the yearly installations of new wind farms employ DFIG. The main advantage of DFIG wind turbine system is cost-effective for an inverter because its rating is typically 25% of rating of total system and the operating speed range of the DFIG is ±33% around the synchronous speed. Approximately 2 to 3% efficiency improvement can be obtained due to the small size of power converters.

A typical configuration of a DFIG system with nonlinear load is shown in figure 1. The stator side of a DFIG is directly connected to the line while the rotor side is fed through two back-to-back power converters with dc link. In order to cover a wide speed range from subsynchronous to supersynchronous speeds, these power converters must be bi-directional power converters.

The dc link capacitor is capable of absorbing the instantaneous power difference between line side and machine side converter. Therefore, these two converters can be separately controlled. The configuration of a PWM voltage source line side converter is shown in figure 2. The function of the line side converter is to regulate the dc bus voltage at a reference value and to ensure that the converter operates at unity power factor. The control technique of the converter is based on the model of the system on the synchronously rotating reference frame (d-q axis) [2], [3]. Steady state balanced sinusoidal three phase voltages and currents, which are transformed onto the d-q axis, become dc values and can be easily controlled by PI controller. The active power and reactive power are decoupled from each other and the power flow between the line and the dc link can be independently controlled.

Today, the increasing use of power electronics equipment causes unbalanced non-sinusoidal currents in the ac supply system. These harmonic currents are the causes of various undesirable phenomena in the power quality such as losses, malfunction of sensitive devices, electromagnetic interference, faulty timing signals, increasing heat and shorten motor life. Normally, active power filters (APF) are used to compensate harmonic currents and reactive current component to improve the power quality. Furthermore, the APF can balance the load currents.

The control methods for rotor side converter of DFIG system with APF operation have been investigated [4] – [6]. The stator currents of the DFIG are controlled by rotor side converter to compensate the harmonic currents. These control schemes produce non-sinusoidal currents in the stator of the machine which can cause negative effect on the DFIG.

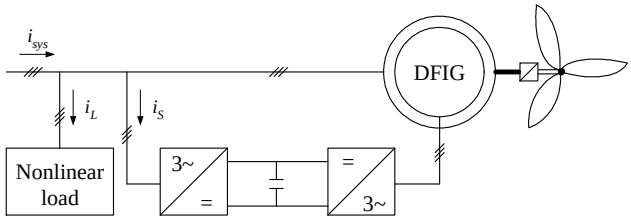

Fig.1. Schematic diagram of DFIG for wind turbine system with nonlinear load.

S. Wangsathitwong (corresponding author) and S. Sirisumrannukul are with King Mongkut's University of Technology North Bangkok (KMUTNB), Bangkok, Thailand. Phone: +66-2-9132500 ext.6304, Fax: +66-2-5874356. E-mail: ssww@kmutnb.ac.th and spss@kmutnb.ac.th.

S. Chatratana is with Technology Management Center, National Science and Technology Development Agency (NSTDA), 111 Thailand Science Park, Paholyothin Rd., Patumthani, Thailand. E-mail: somchaich@nstda.or.th.

W. Deleroi was with Delft University of Technology, Delft, Netherlands. E-mail: werner.deleroi@skynet.be.

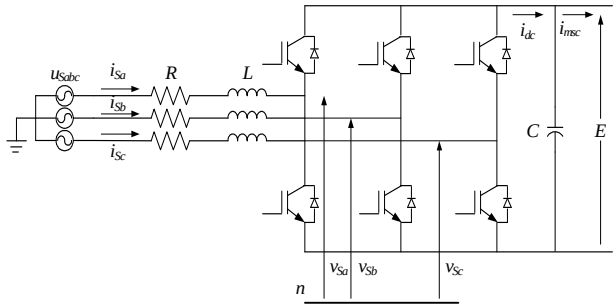

Fig.2. Equivalent circuit of the ac system with line side converter

The control scheme of the line side converter is more flexible. The function of line side converter can be enhanced to operate as a shunt APF to compensate harmonic currents. The line side converter with APF operation will then be capable of simultaneously compensating current harmonics, reactive power and unbalanced load current. The advantage of the proposed method is that the harmonic currents are directly compensated by the converter which would give faster response and better accuracy than the method of compensation through the rotor side converter.

There are several control methods of shunt APF for the application of line side converter with APF [7], [8]. For the synchronously rotating reference frame model, the compensated currents can be directly derived from the real load currents without the need of line voltage information. Furthermore, the reference current signals are not affected by unbalanced voltage or voltage distortion. These advantages increase the robustness of the system and simplify the design of controllers. The harmonic current and reactive power can be separately control by individual control loop [9].

This paper presents a control method of the line side converter for DFIG in conjunction with active power filter and load balancing. The rotor side converter of the DFIG is controlled in the same way as in normal operation while the line side converter is assigned to regulate dc link voltage, to compensate non-sinusoidal currents, to control reactive power and to balance three phase currents. With these functions, the load currents are measured and transformed on to the d-q axis of the synchronously rotating reference frame. The non-sinusoidal, reactive and unbalanced current components are extracted from the d-q components and used as references for currents compensation. Based on this scheme, the line side converter can compensate both the non-sinusoidal currents and unbalanced currents directly.
This paper is organized as follows: The mathematical model of line side voltage source converter and the proposed control method are investigated in Section 2, together with the block diagram of the control system. The simulation results to verify the control performances are shown in Section 3. The conclusion is given in Section 4.

2. MATHEMATICAL MODEL AND CONTROL METHOD

2.1 Nonlinear Model Analysis and Proposed Method

The line side converter is a three phase AC/DC converter which is connected to the three phase power supply on one side with a capacitor on the dc side. The voltage equations of the system are:

$$\begin{bmatrix} u_{Sa} \\ u_{Sb} \\ u_{Sc} \end{bmatrix} = R \begin{bmatrix} i_{Sa} \\ i_{Sb} \\ i_{Sc} \end{bmatrix} + L \frac{d}{dt} \begin{bmatrix} i_{Sa} \\ i_{Sb} \\ i_{Sc} \end{bmatrix} + \begin{bmatrix} v_{Sa} \\ v_{Sb} \\ v_{Sc} \end{bmatrix} \tag{1}$$

The power equation of dc link voltage can be written, as:

$$Ei_{msc} + EC\frac{dE}{dt} = Ei_{dc} = P_{dc} \tag{2}$$

Transforming (1) onto the synchronously rotating reference frame and align d-axis of reference frame with the complex vector of the phase voltage of the supply, results in:

$$u_{Sd} = Ri_{Sd} + L\frac{di_{Sd}}{dt} - \omega Li_{Sq} + v_{Sd} \tag{3}$$

$$u_{Sq} = 0 = Ri_{Sq} + L\frac{di_{Sq}}{dt} + \omega Li_{Sd} + v_{Sq} \tag{4}$$

The three phase instantaneous supply powers are,

$$\begin{aligned} s &= \frac{2}{3} u_{Sdq} i^{*}_{Sdq} \\ &= p + jq \end{aligned} \tag{5}$$

$$p = \frac{2}{3} u_{Sd} i_{Sd} \tag{6}$$

$$q = -\frac{2}{3} u_{Sd} i_{Sq} \tag{7}$$

If the power loss in the converter can be neglected, the instantaneous dc power in (2) and ac power in (6) are the same. Therefore, the dc bus voltage can be controlled via i_{Sd}. The i_{Sd} demand is derived from the dc bus voltage error through a standard PI controller, while i_{Sq}, demand determines the reactive power or power factor on the line side of the converter. The errors of both i_{Sd} and i_{Sq} act as inputs of PI controllers to generate the line side converter terminal voltage reference signal v_{Sd} and v_{Sq}.

For APF application, the nonlinear load currents are transformed onto the d-q axis frame. These two quantities are composed of the dc components and ripples or ac components as described in (8) and (9).

$$i_{Ld} = \bar{i}_{Ld} + \tilde{i}_{Ld} \tag{8}$$

$$i_{Lq} = \bar{i}_{Lq} + \tilde{i}_{Lq} \tag{9}$$

Based on (6) and (7), the dc component of (8) is related to the conventional fundamental active load current whereas the ac component is related to the harmonic currents and the negative sequence of the unbalanced load currents. The compensated d-axis current is calculated by extracting the ac component from the d-axis current. The q-axis load current in (9) represents reactive load current, harmonic current and unbalanced load. In order to avoid negative effects the q-axis load current should be zero. Therefore, the reference currents required by APF to compensate non-sinusoidal load currents, reactive power and unbalanced load current are

$$i_{Ld}^{*} = -\tilde{i}_{Ld} \tag{10}$$

$$i_{Lq}^{*} = -i_{Lq} \tag{11}$$

The compensated d-q axis currents, in (10) and (11), are fed and added to the conventional current controller of the line side converter. The block diagram of the proposed method is shown in figure. 3. The low pass filter is used to extract balanced active power load current, which is in the form of dc current, from d-axis current. Then the harmonic current and unbalanced load current can be determined by subtracting the dc current from the d-axis current.

2.2 Design of Control Loop

The design of both the current loop and dc voltage loop controller can be carried out according to the pole placement method [10]. The process transfer function can be described as the first order model.

$$G_p(s) = \frac{K_p}{1+sT}$$

The transfer function of PI controller is

$$G_c(s) = K\left(1+\frac{1}{sT_i}\right)$$

With simplified block diagram of control in figure 4, the closed loop characteristic equation becomes

$$s^2 + s\frac{1+K_pK}{T} + \frac{K_pK}{TT_i} = 0 \tag{12}$$

The analysis of the characteristic equation shows that the control loop is stable for all positive values of K and T_i [11].

The standard form of second order characteristic equation is

$$s^2 + 2\zeta\omega_n s + \omega_n^2 = 0 \tag{13}$$

Comparing (12) and (13), the controller parameter can then be designed as in (14) and (15).

$$K = \frac{2\zeta\omega_n T - 1}{K_p} \tag{14}$$

$$T_i = \frac{2\zeta\omega_n T - 1}{\omega_n^2 T} \tag{15}$$

The two closed loop poles in (12) can be chosen arbitrarily by assigning the controller constant terms, K and T_i, as in (14) and (15).

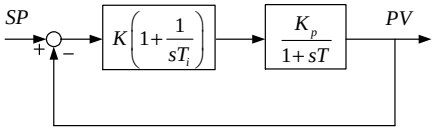

Fig.4. Block diagram of process controller.

It should be noted that the assumption of plant (converter) as a first order system is used in the simplified model. Thus it is obvious that the design of gain and time constant of controller depends on how close is the approximation. However, the results from (14) and (15) are good enough as initial values. Taking into account of dead time of the switches and time delay of the system should improve the design results considerably.

Design of Current Loop

In current control loop, the d-q axis terminal reference voltages in (3) and (4) can be made independent of each other by feeding forward the control components to compensate the two cross coupling terms. As a result, the d-q axis current control loops have been fully decoupled. Then according to (14) and (15), the d-q axis current PI controller parameter can be selected.

$$K_i = 2\zeta\omega_n L - R \text{ and } T_{ii} = \frac{2\zeta\omega_n L - R}{L\omega_n^2} \tag{16}$$

Design of DC Voltage Loop

Similarly, the dc voltage controller parameters can then be designed with the terms in (14) and (15) as in (17).

$$K_v = 2\zeta\omega_n C - 1/R_{dc} \text{ and } T_{iv} = \frac{2\zeta\omega_n C - 1/R_{dc}}{C\omega_n^2} \tag{17}$$

2.3 Linearized Model and Stability Analysis

The nonlinear equations in (2)-(7) can be linearized [12] and the linear control analysis such as stability and design technique can be directly applied. The linear relation between converter terminal voltage, v_S, and dc bus voltage, E, is expressed as

$$v_S = mE \tag{18}$$

Equations (2)-(4) can be rewritten in state-space equations as

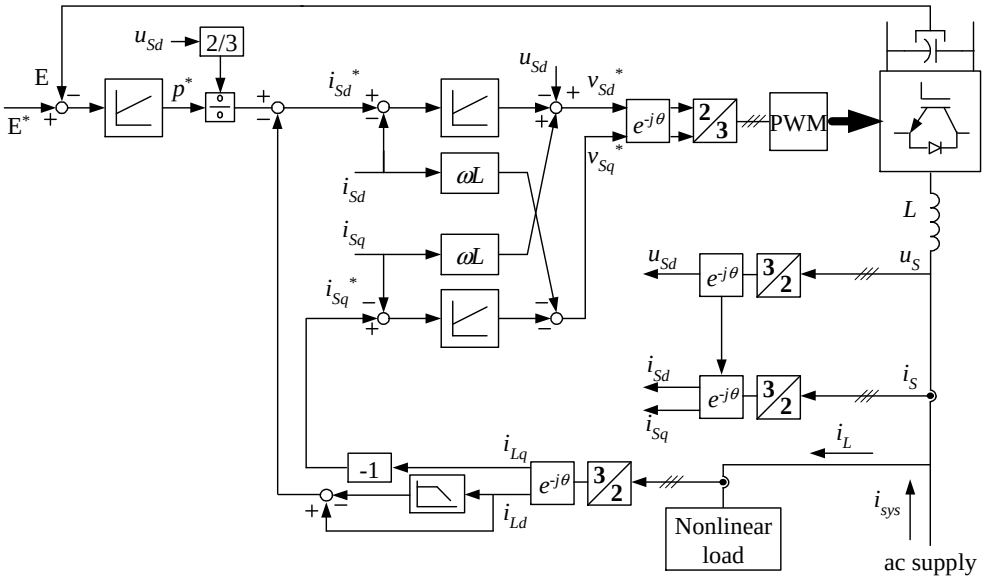

Fig.3. Block diagram of the control system of line side converter with APF and load balancing.

$$L\frac{di_{Sd}}{dt} = -Ri_{Sd} + \omega Li_{Sq} + (u_{Sd} - v_{Sd}) \tag{19}$$

$$L\frac{di_{Sq}}{dt} = -Ri_{Sq} - \omega Li_{Sd} - v_{Sq} \tag{20}$$

$$C\frac{dE}{dt} = i_{dc} - \frac{E}{R_{dc}} \tag{21}$$

If it is assumed that the dc power is equal to converter terminal active power, the expression for the dc power is

$$P_{dc} = Ei_{dc} = \frac{2}{3}v_S(i_{Sd}\cos\delta - i_{Sq}\sin\delta) \tag{22}$$

$$\frac{v_S}{m}i_{dc} = \frac{2}{3}v_S(i_{Sd}\cos\delta - i_{Sq}\sin\delta)$$

$$i_{dc} = \frac{2}{3}m(i_{Sd}\cos\delta - i_{Sq}\sin\delta) \tag{23}$$

Rearranging (19) – (23) in the standard form results in

$$\frac{d}{dt}\begin{bmatrix} i_{Sd} \\ i_{Sq} \\ E \end{bmatrix} = \begin{bmatrix} -\frac{1}{T_S} & \omega & -\frac{m}{L}\cos\delta \\ -\omega & -\frac{1}{T_S} & \frac{m}{L}\sin\delta \\ \frac{2}{3}\frac{m}{C}\cos\delta & -\frac{2}{3}\frac{m}{C}\sin\delta & -\frac{1}{T_{dc}} \end{bmatrix}\begin{bmatrix} i_{Sd} \\ i_{Sq} \\ E \end{bmatrix} + \begin{bmatrix} \frac{1}{L} & 0 \\ 0 & \frac{1}{L} \\ 0 & 0 \end{bmatrix}\begin{bmatrix} u_S \\ 0 \end{bmatrix} \tag{24}$$

$$\frac{d}{dt}\begin{bmatrix} \Delta i_{Sd} \\ \Delta i_{Sq} \\ \Delta E \end{bmatrix} = \begin{bmatrix} -\frac{1}{T_s} & \omega & -\frac{m_0}{L}\cos\delta_0 \\ -\omega & -\frac{1}{T_s} & \frac{m_0}{L}\sin\delta_0 \\ \frac{1}{2}\frac{m_0}{C}\cos\delta_0 & -\frac{1}{2}\frac{m_0}{C}\sin\delta_0 & -\frac{1}{T_{dc}} \end{bmatrix}\begin{bmatrix} \Delta i_{Sd} \\ \Delta i_{Sq} \\ \Delta E \end{bmatrix} + \begin{bmatrix} \frac{m_0}{L}E_0\sin\delta_0 & -\frac{E_0}{L}\cos\delta_0 \\ \frac{m_0}{L}E_0\cos\delta_0 & \frac{E_0}{L}\sin\delta_0 \\ -\frac{1}{2}\frac{m_0}{C}(i_{Sd0}\sin\delta_0 + i_{Sq0}\cos\delta_0) & \frac{1}{2C}(i_{Sd0}\cos\delta_0 - i_{Sq0}\sin\delta_0) \end{bmatrix}\begin{bmatrix} \Delta\delta \\ \Delta m \end{bmatrix} \tag{25}$$

where $T_s = \frac{L}{R}$ and $T_{dc} = R_{dc}C$.

The linearization for small perturbation is represented by the first order terms of Taylor's expansion given in (24). The linear difference equations are given in (25). Therefore, the characteristic equation is

$$\lambda^3 + \left(\frac{2}{T_S} + \frac{1}{T_{dc}}\right)\lambda^2 + \left(\frac{2}{T_S T_{dc}} + \frac{1}{T_S^2} + K + \omega^2\right)\lambda + \left(\frac{1}{T_S^2 T_{dc}} + \frac{K}{T_S} + \frac{\omega^2}{T_{dc}}\right) = 0 \tag{26}$$

when $K = \frac{1}{2}\frac{m_0^2}{LC}$

It can be seen that there is no δ term in the characteristic equation. Thus switching angle does not affect the position of characteristic roots. Reassigning the coefficients of the polynomial in terms of a_0, a_1 an a_2, (26) gives:

$$\lambda^3 + a_2\lambda^2 + a_1\lambda + a_0 = 0$$

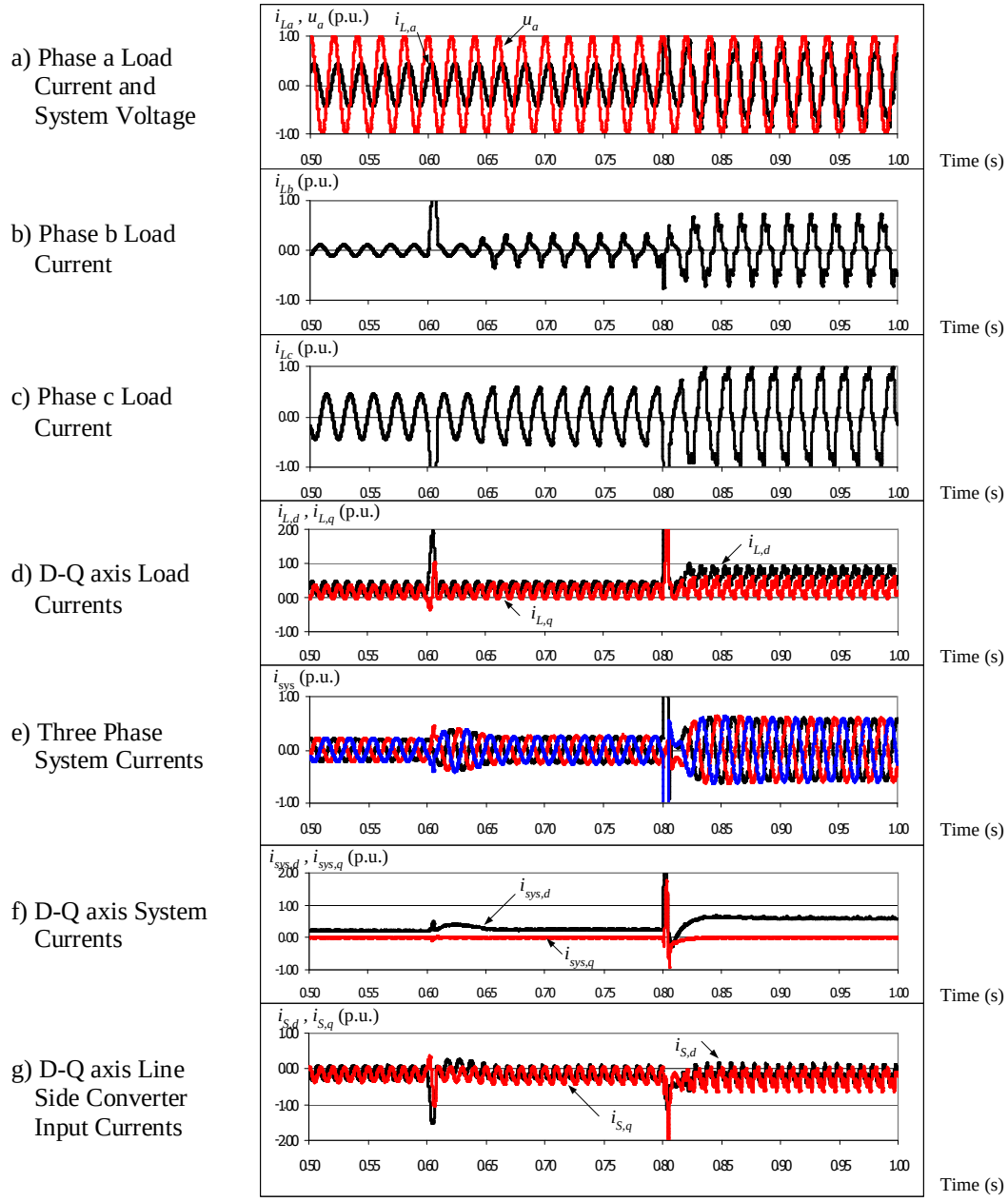

Fig.5. Simulation results of the proposed method.

The Routh-Hurwitz criterion can be used to determine stability analysis of this system.

$$\begin{array}{c|cc} \lambda^3 & 1 & a_1 \\ \lambda^2 & a_2 & a_0 \\ \lambda^1 & a_1 - a_0 / a_2 & \\ \lambda^0 & a_0 & \end{array}$$

For the system to be stable, the component of Routh array in the λ^1 row must be greater than 0, which results in

$$\frac{4}{T_S} + \frac{2}{T_{dc}} + \frac{2T_{dc}}{T_S^2} + KT_{dc} + KT_S + 2\omega^2 T_{dc} \geq 0 \qquad (27)$$

Obviously, for all positive values of system parameters the system is stable.

3. SIMULATION RESULTS

The proposed method was simulated with the circuit in Fig. 1, to verify the control performances of the system. The test conditions were started by applying linear unbalanced load with lagging power factor at t = 0.0 sec. At t = 0.6 sec a single phase nonlinear load was connected between phase b and phase c. The nonlinear effect was increased by additional three phase nonlinear load at t = 0.8 sec. The responses of the load currents (i_{Labc}), the ac system currents (i_{sys}) and the compensation currents (i_S) are shown in figure 5. Note that the waveforms of steady state load currents (i_L) in figure 5a, 5b and 5c from t = 0.5 to 0.6 sec are unbalanced sinusoidal with lagging power factor. During this period,

figure 5d shows that there are ac components in both d-q axis currents. For compensation currents (i_S) in figure 5g, the d-axis current of the system becomes dc value with zero q-axis current. The q-axis current in fact remains zero all the times which indicates unity power factor operation of the converter. The three phase currents of the system (i_{sys}) are balanced as shown in figure 5e.

When the nonlinear load is connected between phase b and c at t = 0.6 sec. and the control system responded in less than 0.1 sec (figure 5e). Figures 5a – 5c show the increase in nonlinear three phase loads at t = 0.8 sec. The control system increases the compensated currents accordingly as shown in Figure 5g. After short transients the system recovers back to balanced operation with sinusoidal currents at unity power factor which are shown in figure 5e and 5f. The performance of the line side converter with APF are clearly indicated in figures 5e and 5f with three phase system currents and d-q axis currents for both steady state and dynamic behaviors. It can be seen that the system currents remain sinusoidal, balanced and lower than load currents. As a result, d-q axis system currents are constant due to the compensated current from the line side converter in figure 5g. The negative d-axis current in Figure 5g at t = 0.8 sec indicates that the line side converter is in generating mode for a short time.

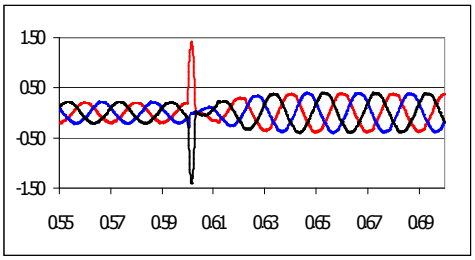

Fig.6. Three phase system current without reactance error.

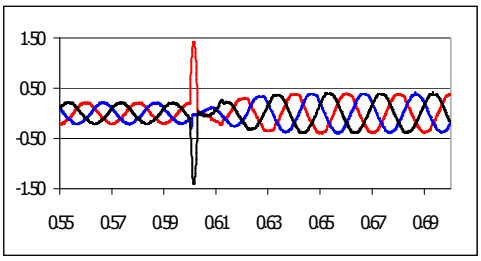

Fig.7. Three phase system current with reactance err

The robustness of proposed control system of the line side converter has been tested by keeping all the parameters of the controllers fixed, but reducing the reactance of the filter whose value is used in the feed forward component of current control loop by 10% of its original value. The original system and the system with reactance error were tested with the same operating conditions and with the linear unbalanced loads were connected to the system. At t = 0.6 sec the balanced nonlinear load are switched on. The results are shown in Figure 6 for the response of the original system and in Figure 7 for the system with reactance error, respectively. It can be seen that both responses are nearly the same even with large error of the reactance value.

4. CONCLUSION

The control of line side converter with active power filter and load balancing capability for DFIG has been demonstrated. The control scheme is based on the model of the system on synchronously rotating reference frame (d-q axis). It was proposed that the elimination of ac component of the d-axis current and q-axis current by appropriate compensation ensures that the converter is operating at unity power factor with active power filter function and load balancing capability. The potential benefit of the proposed method is the combination the active power filter function and load balancing function in a single converter. From the simulation results, the system was proved to be able to operate with balanced sinusoidal current waveforms and at unity power factor even when it was connected to the unbalanced nonlinear loads. The loading capability of the system is increased due to supply system currents are lower than load currents. The overall system efficiency is improved owing to the absence of harmonic currents and reactive current.

NOMENCLATURE

C	DC bus capacitance
E	DC bus voltage
i_{dc}	DC bus current
$\bar{i}_{Ldq}$	DC component of d-q axis load currents
$\tilde{i}_{Ldq}$	AC component of d-q axis load currents
i_{msc}	Machine side converter dc current
i_{Sabc}	Three phase line side converter input currents
i_{Sdq}	D-Q axis line side converter input currents
i_{sys}	Three phase system currents
$i_{sys,dq}$	D-Q axis system currents
K, K_p	Controller and process gain
L	Line side filter inductance
m	Proportional factor
p, q	Instantaneous line side converter input active power and reactive power, respectively
P_{dc}	DC bus power
R	Line side filter resistance
R_{dc}	DC equivalent resistance
s	Instantaneous line side converter input apparent power
T	Process time constant
T_{dc}	DC bus time constant
T_i	Controller integral time
T_s	Line side filter time constant
u_{Sabc}	Three phase system voltages
u_{Sdq}	D-Q axis system voltages
v_S,	Fundamental component of line side converter instantaneous voltage

v_{Sabc} Three phase line side converter terminal voltages

v_{Sdq} D-Q axis line side converter terminal voltages

θ Reference angle in synchronously rotating reference frame

ω System voltage frequency

δ Line side converter terminal voltage phase angle

REFERENCES

[1] Ackerman, T. 2005. *Wind Power in Power System. Chichester*. John Wiley & Sons.

[2] Pena, R. Clare, J.C. and Asher, G.M. 1996. Doubly fed induction generator using back-to-back converter and its application to variable-speed wind-energy generation. *IEE Proc.-Electr. Power Appl.*, vol. 143, no. 3, pp. 231-241.

[3] Leonhard, W. 1996. *Control of Electrical Drive*. Berlin German: Springer.

[4] Toufik, B. Machmoum, M. and Poitiers, F. 2005. Doubly fed induction generator with active filtering function for wind energy conversion system. In *Proceedings of Power Electronics and Application Conference*. 11-14 September.

[5] Jain, A. K. Ranganathan and V. T. 2008. Wound rotor induction generator with sensorless control and integrated active filter for feeding nonlinear loads in a stand-alone grid. *IEEE Trans. Ind. Electron.*, vol. 55, no. 1, pp. 218-228.

[6] Abolhassani, M. T. Enjeti, P and Toliyat, H. 2008. Integrated doubly fed electric alternator/active filter (IDEA), a viable power quality solution, for wind energy conversion systems. *IEEE Trans. Energy Convers*., vol. 23, no. 2, pp. 642-650.

[7] Akagi, H. Watanabe, E. H. Aredes, M. 2007. *Instanneous Power Theory and Aplications to Power Conditioning*. IEEE Press.

[8] Chen, D. Xie, S. 2004. Review of the control strategies applied to active power filters. In *Proceedings of Electric Utility Deregulation, Restructuring and Power Technologies Conference*. April.

[9] Tremblay, E. Chandra, A and Lagace, P. J. 2006. Grid-side converter of DFIG wind Turbines to enhance power quality of distribution network. In *Proceedings of Power Engineering Society General Meeting*. 18-22 June.

[10] Astrom, K. J. Hagglund, T. 1995. PID Controller: Theory, Design, and Tuning. Instrument Society of America.

[11] Rashid, M. H. 2001. *Power Electronics Handbook*. Academic Press.

[12] Voraphonpiput, N. and Chatratana, S. 2004. STATCOM Analysis and Controller Deesign for Power System Voltage Regulation. In *Proceedings of Transmission and Distribution Conference*. Dalian, China, 1-6.